2011 50th IEEE Conference on Decision and Control and
European Control Conference (CDC-ECC)
Orlando, FL, USA, December 12-15, 2011

A Nonlinear Estimator for Dynamical and Robust Sensorless Control of Permanent Magnet Synchronous Machines

Jean-François Stumper, Dirk Paulus and Ralph Kennel, *Senior Member*, *IEEE*

***Abstract*— This paper proposes an angular position and speed estimation scheme that is based on a direct evaluation of the angle of the voltage induced by the spinning rotor (back-EMF) of a permanent-magnet synchronous motor (PMSM). It is an inverse parallel-model estimation method, meaning the rotor position and speed are directly calculated based on stator current measurements and the stator voltage commands. In contrast to existing schemes, no observer, no integration and no speed or flux estimation is necessary. The estimators are extended with filters to cope with measurement noise, and directly used for field-oriented control. It is shown algebraically and experimentally that parametric robustness is outstanding. The resulting estimated angle is driftless even under uncertainties. The scheme is suitable for encoderless control of a PMSM at high and low speeds. The performance of the scheme is confirmed by experimental results.**

I. Introduction

For field-oriented control of a permanent-magnet synchronous motor (PMSM), the mechanical rotor position as well as information on the current components are required. In contrast to the current measurement, which is done directly at the inverter, the position information has to be measured at the motor, inheriting a strong disadvantage if for instance a high distance to the power electronics is necessary. The position measurement is very expensive and fault sensitive. Sensorless methods avoid the need for a mechanical sensor, bringing considerable advantages in cost and robustness.

Two principles for sensorless control can be divided, separated by their applicable operational domain. The first one is based on evaluation of the voltage induced by the spinning rotor (back-EMF), first presented in [1]. Further developments of this method are shown in [2]. As the induced voltage is proportional to the speed, the information obtained by the method vanishes at low speed. In the low speed domain, saliency-based methods dominate [3] [4]. This scheme offers disadvantages in high speed and requires special magnetic characteristics of the motor. To cover the whole speeed range, usually, hybrid methods are used which combine both principles [5], or feedforward control is applied at low speed if accuracy is not that important [6].

From control theoretical standpoint, back-EMF methods are more interesting as theoretical developments can improve behavior, while injection schemes are based on the given physics of a PMSM. Still, in-depth theoretical studies are quite rare, even though the results give important insight [6] [7]. A major reason for misfunction are paramter deviations, several back-EMF methods aim at reducing this impact. [8] shows an adaptive sliding mode approach with a parameter compensation method, the effect of parameter deviations is also shown.

Furthermore, a look at the induction motor is also very interesting, even though the problem of sensorless control is different. Asymptotic observers have problems in the low-speed area, the integration results in a drift, and a filter is used as solution. This results in a speed offset at low speed. Only relatively fast speed reversals with low load are possible with the conventional asymptotic observers. However, as motivation to research on estimators, it was shown that it is well possible to operate an estimator at low and zero speed [9] [10] [11]. The key to this result is the avoidance of an integration of the stator model, the current measurements are derived instead.

In this contribution, a back-EMF-based position estimation scheme is introduced that is based on a parallel-model estimator. The control structure is changed to avoid some disadvantages. With the new estimation structure, the impact of parametric uncertainties is reduced, and dynamical operation is improved.

The scheme presented in this paper combines two recent improvements proposed for back-EMF methods for PMSMs. The first is the estimation of the position without speed estimation [7]. The position can be estimated with the back-EMF angle, whereas the speed is proportional to the back-EMF magnitude, which is, however, very sensitive to uncertainties. This way, parametric robustness is improved. The second is the direct estimation of the position without the use of an asymptotic observer [12] [13]. Then, there is no more need for observer gain tuning. As further development of this paper, which is the complete avoidance of the integration, the mentioned drift problems do not appear and do not require any consideration. Preliminary results were presented in [14]

II. Parallel Models: An Alternative State Estimation Technique

Usually, for a linear control system, described by the dynamical equations

$$\dot{\boldsymbol{x}} = \boldsymbol{A}\boldsymbol{x} + \boldsymbol{B}\boldsymbol{u}, \tag{1}$$

an asymptotic observer is applied if some of the states $\boldsymbol{x}$ are required for control, but not measurable. On the underlying example of a permanent-magnet motor, the currents are measured, as these measurements are also required for safe operation of the power conversion stage. The position and speed are not measured in sensorless control. The conventional method is to design an asymptotic observer, consisting of a state-space system

$$\dot{\tilde{\boldsymbol{x}}} = \hat{\boldsymbol{A}}\tilde{\boldsymbol{x}} + \hat{\boldsymbol{B}}\boldsymbol{u} + \boldsymbol{K}(\boldsymbol{x}_m - \tilde{\boldsymbol{x}}), \tag{2}$$

where $\tilde{\boldsymbol{x}}$ is the observed state, $\boldsymbol{x}_m$ are the measured states, $\hat{\boldsymbol{A}}$ and $\hat{\boldsymbol{B}}$ the model parameters and $\boldsymbol{u}$ the (commanded) control input. There are feedback gains $\boldsymbol{K}$ which are to be tuned. Furthermore, as the dynamics of the complete system are augmented (i.e. the order of the system is increased by the number of observed states), it must be guaranteed that these additional dynamics are not destabilizing, even under model parameter offsets. For the underlying application, this is quite difficult, as the model parameters are uncertain: the inductances vary with the operation point because of magnetic saturation, while the resistance and the permanent magnet flux vary with temperature. As a general result, $\boldsymbol{K}$ must be designed quite small such that these errors do

This work was supported through the National Research Funds of Luxembourg under grant PhD-08-070.

The authors are with the Department of Electrical Engineering and Information Technology, Technische Universität München, Arcisstr. 21, D-80333 Munich, Germany. jean-francois.stumper@tum.de dirk.paulus@tum.de

not destabilize the system, inheriting quite slow observer convergence and therefore less dynamical operation.

An alternative to asymptotic observers are parallel-model estimators. The state vector $\boldsymbol{x}$ is decomposed into the measured states $\boldsymbol{x}_m$ and the unmeasured states $\boldsymbol{x}_u$ (to be estimated), therefore $\boldsymbol{x} = (\boldsymbol{x}_m, \boldsymbol{x}_u)^{\mathrm{T}}$. Only the relevant rows of the system description (1) are used, denoted by $\boldsymbol{A}_m$ resp. $\boldsymbol{B}_m$. Then, the dynamical equation

$$\dot{\boldsymbol{x}}_m = \hat{\boldsymbol{A}}_m \boldsymbol{x} + \hat{\boldsymbol{B}}_m \boldsymbol{u}, \tag{3}$$

follows directly from (1). The next task is to extract the unmeasured states $\hat{\boldsymbol{x}}_u$ to obtain the estimator equation(s)

$$\hat{\boldsymbol{x}}_u = \boldsymbol{\alpha}(\hat{\boldsymbol{A}}_m, \hat{\boldsymbol{B}}_m, \boldsymbol{u}, \boldsymbol{x}_m, \dot{\boldsymbol{x}}_m) \tag{4}$$

which is a so-called inverse parallel-model estimator. This estimator is based on (physical) model parameters, measurements and control input commands, and does not require tuning of any feedback gain. It can therefore be assumed simpler to implement and represents a drastic design change compared to an asymptotic observer. However, some problems become obvious:

- The measured state derivatives $\dot{\boldsymbol{x}}_m$ must be calculated. As this is noncausal and as the measurements are usually noisy, this requires extensive filtering and inherits phase lag, resulting in poor performance.
- How can $\hat{\boldsymbol{x}}_u$ be extracted? This is not easy, even if the unmeasured states are observable. There are usually several ways to obtain some function $\boldsymbol{\alpha}(\cdot)$.
- What is the impact of parameter offsets in $\hat{\boldsymbol{A}}$ and $\hat{\boldsymbol{B}}$?

The questions can be answered with some results from control theory, notably from flatness-based control. It is shown that the conventional state representation for PMSMs is problematic, but that for instance a polar state representation makes calculation of $\dot{\boldsymbol{x}}_m$ quite easy. Extraction of $\hat{\boldsymbol{x}}_u$ is then also simplified, two nice and independent equations are found for the position and the speed. The robustness towards parameter offsets can be shown to be very good, and the scheme is driftless, unlike integration schemes. It can therefore be implemented without tuning, a simplification to the state of the art.

III. Direct Back-EMF Estimation in Polar Stator-Current Coordinates

A. Transformed Fundamental Model

A coordinate transformation of the current space vector to polar coordinates is proposed [15] with vector length

$$\rho = \sqrt{i_\alpha^2 + i_\beta^2} \tag{5}$$

as well as the vector angle

$$\phi = \begin{cases} \arctan \frac{i_\beta}{i_\alpha} & i_\alpha \geq 0 \\ \arctan \frac{i_\beta}{i_\alpha} + \pi & i_\alpha < 0 \end{cases}, \tag{6}$$

which is in the domain $\phi \in [0, 2\pi]$. This transformation is not based on motor parameters, and is valid for a nonzero current vector length $\rho > 0$. One can show that at the points $i_\alpha = 0$ the transformation is continuous, as

$$\lim_{i_\alpha \to 0^-} \phi = \lim_{i_\alpha \to 0^+} \phi \tag{7}$$

for both cases $i_\alpha < 0$ and $i_\alpha > 0$. The inverse transformation is

$$i_\alpha = \rho \cos\phi, \tag{8}$$
$$i_\beta = \rho \sin\phi. \tag{9}$$

The motor model in transformed coordinates is given as

$$\begin{cases} L\dot{\rho} & = -R\rho + K\omega_M \sin(n_p\varphi_M - \phi) + u_P \\ L\rho\dot{\phi} & = -K\omega_M \cos(n_p\varphi_M - \phi) - u_O \\ J\dot{\omega}_M & = -K\rho \sin(n_p\varphi_M - \phi) - \tau_L \\ \dot{\varphi}_M & = \omega_M \end{cases}, \tag{10}$$

where the voltage space vector is transformed to

$$u_P = u_\alpha \cos(\phi) + u_\beta \sin(\phi), \tag{11}$$
$$u_O = u_\alpha \sin(\phi) - u_\beta \cos(\phi), \tag{12}$$

for a concise notation. The voltage vector components u_P and u_O are the parallel respectively orthogonal projections to the current vector $(i_\alpha, i_\beta)^T$. It is noted that the transformed model is only valid for $\rho \neq 0$, inherited from the coordinate transformation.

B. Direct Position Estimation

Extraction of φ_M is possible in a straightforward manner with the differential equations in the current

$$K\omega_M \sin(n_p\varphi_M - \phi) = L\dot{\rho} + R\rho - u_P, \tag{13}$$
$$K\omega_M \cos(n_p\varphi_M - \phi) = -L\rho\dot{\phi} - u_O, \tag{14}$$

with the definition of the $\tan = \frac{\sin}{\cos}$ function. From the transformed model, it can be seen that $n_p\varphi_M - \phi \neq 0$ if the motor torque τ_M is nonzero, and $n_p\varphi_M - \phi \neq \frac{\pi}{2}$ if there is a nonzero field-generating d-current.

The term $K\omega_M$ is extracted from these equations

$$K\omega_M = \frac{L\dot{\rho} + R\rho - u_P}{\sin(n_p\varphi_M - \phi)} = \frac{-L\rho\dot{\phi} - u_O}{\cos(n_p\varphi_M - \phi)}, \tag{15}$$

which, in contrast to the corresponding equation in the previous section, is valid over the whole angular range φ_M if the current magnitude ρ is nonzero. To ensure $\rho \neq 0$ in all operation points, it is set $i_d = i_{d0}^* = 0.05$ p.u.

The estimation equation of the electrical angle $\varphi_e = n_p\varphi_M$ is based on measurements on ϕ, ρ, u_P and u_O, on the derivatives $\dot{\phi}$ and $\dot{\rho}$, as well as on the uncertain parameters $\hat{L}$ and $\hat{R}$

$$\bar{\varphi}_e = -\arctan\left(\frac{\hat{L}\dot{\rho} + \hat{R}\rho - u_P}{\hat{L}\rho\dot{\phi} + u_O}\right) + \phi, \tag{16}$$

and the case differentiation

$$\hat{\varphi}_e = \begin{cases} \bar{\varphi}_e & \text{if } (-\hat{L}\rho\dot{\phi} - u_O) \geq 0 \\ \bar{\varphi}_e + \pi & \text{if } (-\hat{L}\rho\dot{\phi} - u_O) < 0 \end{cases}, \tag{17}$$

which is the main equation of this contribution. The motor constant K and the speed ω_M are eliminated, and the estimation is based exclusively on stator parameters and stator variable measurements.

C. Direct Speed Estimation

In same manner a speed estimator can be realized. The trigonometric terms are extracted from the current equations in (10), and with $\sin^2(x) + \cos^2(x) = 1$, the speed ω_M is found by

$$\bar{\omega}_M = \frac{1}{K}\sqrt{(\hat{L}\dot{\rho} + \hat{R}\rho - u_P)^2 + (\hat{L}\rho\dot{\phi} + u_O)^2}, \tag{18}$$

and the case differentiation

$$\hat{\omega}_M = \begin{cases} \bar{\omega}_M & \text{if } \frac{\hat{L}\dot{\rho} + \hat{R}\rho - u_P}{\sin(n_p\varphi_M - \phi)} \geq 0 \\ -\bar{\omega}_M & \text{if } \frac{\hat{L}\dot{\rho} + \hat{R}\rho - u_P}{\sin(n_p\varphi_M - \phi)} < 0 \end{cases}. \tag{19}$$

An alternative to this algebraic estimator would be an approximated derivative of the estimated position, for instance by an asymptotic filter [7]. Combined with this position estimator, however, the resulting signal is very noisy, especially in low speed.

IV. Analysis: Sensitivity, Noise and Stability

For the underlying robustness analysis, the estimated angle is compared to the real angle. The flatness property is exploited and the estimated angle, determined by the estimation equation with the unsafe parameters $\hat{L}$ and $\hat{R}$, is subtracted from the original angle, determined by the exact parameters and the original current.

A. Impact of Parametric Uncertainties

The inductance $\hat{L}$ is not exactly known, therefore in the estimator, an approximated value

$$\hat{L} = L + \Delta L \tag{20}$$

is applied. The value ΔL represents the absolute uncertainty of the parameter. The offset of the estimated angle φ_M

$$\Delta\varphi_M = \hat{\varphi}_M - \varphi_M \tag{21}$$

can be directly evaluated using the flatness parameterization. With $\arctan(x) - \arctan(y) = \arctan((x-y)/(1+xy))$ and some further developments, the result simplifies to

$$\Delta\varphi_M = \frac{1}{n_p}\arctan\left(\frac{\Delta L\, c_{L1}}{\Delta L\, c_{L2} + c_{L3}}\right), \tag{22}$$

with

$$c_{L1} = -u_O\dot{\rho} + \rho\dot{\phi}(R\rho - u_P), \tag{23}$$
$$c_{L2} = \rho\dot{\phi}(L\rho\dot{\phi} + u_O) + \dot{\rho}(L\dot{\rho} + R\rho - u_P), \tag{24}$$
$$c_{L3} = (L\rho\dot{\phi} + u_O)^2 + (L\dot{\rho} + R\rho - u_P)^2. \tag{25}$$

The same procedure is repeated to compute the influence of stator resistance uncertainty

$$\hat{R} = R + \Delta R, \tag{26}$$

which affects the estimated angle by

$$\Delta\varphi_M = \frac{1}{n_p}\arctan\left(\frac{\Delta R\, c_{R1}}{\Delta R\, c_{R2} + c_{R3}}\right), \tag{27}$$

with

$$c_{R1} = \rho(L\rho\dot{\phi} + u_O), \tag{28}$$
$$c_{R2} = \rho(L\dot{\rho} + R\rho - u_P), \tag{29}$$
$$c_{R3} = (L\rho\dot{\phi} + u_O)^2 + (L\dot{\rho} + R\rho - u_P)^2. \tag{30}$$

Thus the impact of parametric uncertainties are explicitly known.

B. Position Offset in Steady-State

In steady-state, the position error can be explicitly computed. The sensitivity equations (22) and (27), with the results of the previous paragraph, simplify to

$$\Delta\varphi_e = \arctan\left(\frac{n_p\rho\sin(n_p\varphi_M - \phi)\Delta L}{n_p\rho\cos(n_p\varphi_M - \phi)\Delta L - K/n_p}\right), \tag{31}$$

$$\Delta\varphi_e = \arctan\left(\frac{-\rho\cos(n_p\varphi_M - \phi)\Delta R}{\rho\sin(n_p\varphi_M - \phi)\Delta R - K\omega_M}\right), \tag{32}$$

which in field-oriented coordinates can be further simplified with $(n_p\varphi_M - \phi) = \arctan(i_q/i_d)$.

Eqs. (31) and (32) are now verified by measurements. The results are shown on Fig. 1. It is remarked that 300 rpm is a quite low speed, and that for all higher speeds the estimation offset regarding ΔR is lower. Furthermore, the estimation error is naturally dependent on the current magnitude ρ and therefore also of the load torque. It is seen that the open-loop measurements confirm the equations quite well. The closed-loop measurements are, however, different, as the current vector (i_d, i_q) used for the equation is only a reference value and as the real values are influenced by the estimation error $\Delta\varphi_e$.

As a result, the proposed estimation scheme is *very robust towards parametric uncertainties*. A parametric deviation of a multiple of the rated value is necessary until a significant offset appears.

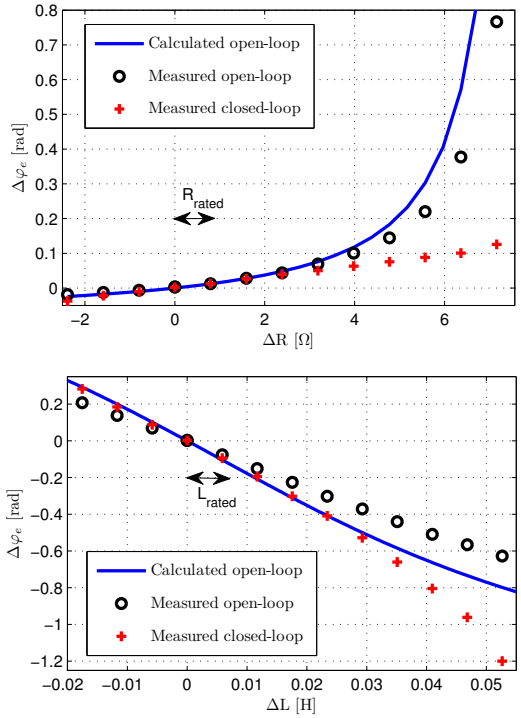

Fig. 1. Top: Sensitivity towards resistance uncertainty ΔR. Bottom: Sensitivity towards inductance uncertainty ΔL. Blue line: calculated value, black circles: measured results in open-loop, red cross: measured results in closed-loop operation. Operating conditions: steady state $\omega_M = 0.1$ p.u. (300 rpm), 0.5 rated torque, reference $(i_d^*, i_q^*) = (0.05, 0.5)$ p.u., $R_{\text{rated}} = 0.86\Omega$, $L_{\text{rated}} = 7$ mH.

C. Measurement Noise

As the position and speed are estimated directly from measurement signals, the impact of measurement noise must be analyzed.

A model in polar stator-current coordinates (10) was chosen which is advantageous regarding the required derivatives. In steady-state, the mechanical speed ω_M and the load torque τ_L are constant. Furthermore, if the system is assumed stable, the currents in field-oriented coordinates i_d and i_q are constant, and thus

$$\dot{\rho} = 0. \tag{33}$$

Then, as follows from the torque equation in (10), the expression $\sin(\varphi_e - \phi)$ is constant too and

$$\dot{\phi} = \dot{\varphi}_e = \omega_e. \tag{34}$$

Therefore, the current derivatives that are required for position and speed estimation are both constant in steady state. Only in transient operation, these derivatives vary. Therefore, regarding steady-state operation, it is acceptable

to apply first-order low-pass filters along with approximated differentiation of the current signals

$$\dot{\rho} \approx \frac{s}{T_{LP}s+1}\,\rho, \tag{35}$$

respectively

$$\dot{\phi} \approx \frac{s}{T_{LP}s+1}\,\phi, \tag{36}$$

where s is the Laplace operator. The time constant of the low-pass filters T_{LP} has to be lower than the time constant of the currents, otherwise the back-EMF estimation is affected. The time constant of the closed current control loop is $\tau_i \approx \frac{L}{R+K_P}$, where K_P is the gain of the P controller, thus, the controllers must be set moderate. In most electrical drives, however, the sampling rate of the control system is much higher than the current time constants. For instance, in the experimental setup, the uncontrolled time constant is $\frac{L}{R} \approx 5$ ms, the closed-loop time constant is $\frac{L}{R+K_P} \approx 1$ ms and the sampling interval is $\Delta T = 0.0625$ ms, thus they have a ratio of 80 respectively 16. For example, it can be chosen $T_{LP} = 0.5$ ms.

As a result, low-pass filters will be sufficient to remove the greatest part of the measurement noise whilst only marginally affecting the accuracy in transient phase, and not affecting the accuracy at all in steady-state.

D. Filters for the Estimator Outputs

For closed-loop encoderless field-oriented control of the synchronous motor, further filtering is necessary. The estimator outputs position and speed vary much slower than the electrical variables, thus, low-pass filters can be used to reduce the noise sensitivity.

For the estimated position, a second order tracking-type filter is applied. It has the characteristic that a constantly increasing signal is not subjected to a phase lag, thus in steady state, as $\varphi_M = \omega_M t$, this filter will not affect the position information. It significantly reduces the influence of the noise and the current controller jerk. The equations are

$$\frac{\mathrm{d}}{\mathrm{dt}} z = -v_1(\tilde{\varphi}_e - \hat{\varphi}_e), \tag{37}$$

$$\frac{\mathrm{d}}{\mathrm{dt}} \tilde{\varphi}_e = z - v_2(\tilde{\varphi}_e - \hat{\varphi}_e), \tag{38}$$

with z as intermediate variable. The feedback gains are chosen as $v_1 = 16000$ and $v_2 = 253$, such that the poles are real and both time constants are 8 ms. The time constant is designed to limit the worst-case phase shift. If the maximum system acceleration c is known, the maximum phase shift will be

$$\Delta\varphi_e \approx n_p \frac{c}{v_1}, \tag{39}$$

which is to be considered as the maximum error is limited.

For the estimated speed $\hat{\omega}_M$, a first-order low-pass filter with a time constant of 2 ms is sufficient.

E. Stability of estimation/control scheme

Foremost, from (16) it can be seen that the estimated and unfiltered position signal $\hat{\varphi}_e$ is not based on any previous estimation results. The position estimate is available almost immediately, except for the very small phase lag caused by the current derivative calculation. For stability consideration, therefore, only the tracking filter (42), (43) and the current and speed controllers are relevant. A misestimation, caused for instance by missing initial rotor position information, does not affect $\hat{\varphi}_e$. One major reason for this is also that position and speed are estimated independently.

The angular error is given as

$$e_\varphi = \varphi_e - \tilde{\varphi}_e. \tag{40}$$

For simplicity assume P control to reduce the order of dynamics, the current controllers which operate in the estimated $(\tilde{d}, \tilde{q})$ frame is then given as

$$\boldsymbol{u}_{\tilde{d}\tilde{q}} = K_P(\boldsymbol{i}^*_{dq} - \boldsymbol{i}_{\tilde{d}\tilde{q}}). \tag{41}$$

The voltage commands are related to the real frame by

$$\boldsymbol{u}_{dq} = \begin{pmatrix} \cos(e_\varphi) & -\sin(e_\varphi) \\ \sin(e_\varphi) & \cos(e_\varphi) \end{pmatrix} \boldsymbol{u}_{\tilde{d}\tilde{q}} = \boldsymbol{Q}\boldsymbol{u}_{\tilde{d}\tilde{q}}. \tag{42}$$

By replacing the voltage commands in the (d, q) model, one obtains

$$L\frac{\mathrm{d}}{\mathrm{dt}}\boldsymbol{i}_{dq} = \begin{pmatrix} -R & n_p\omega_M L \\ -n_p\omega_M L & -R \end{pmatrix} \boldsymbol{i}_{dq} - \begin{pmatrix} 0 \\ K\omega_M \end{pmatrix} + \boldsymbol{Q}^{-1}K_P(\boldsymbol{i}^*_{dq} - \boldsymbol{Q}\boldsymbol{i}_{dq}). \tag{43}$$

The angular error e_φ therefore does not affect the characteristics of the current dynamics. The only impact of e_φ is that the current references $\boldsymbol{i}^*_{dq}$ are applied to the $(\tilde{d}, \tilde{q})$ frame, rotated by e_φ around the intended current references. Therefore stability is not affected by an error e_φ. It results in a performance loss, however, as less torque is generated due to the misalignment. In the next section, current reference compensation is proposed to attenuate this problem.

Now the speed control loop is analyzed. The tracking filter will generate an error e_φ during acceleration. If this error is opposed to the real acceleration the scheme could possibly destabilize. Assuming that the current references are well tracked in the $(\tilde{d}, \tilde{q})$ frame, the mechanical equation of the rotor is

$$J\frac{\mathrm{d}}{\mathrm{dt}}\omega_M = Ki_q - \tau_L \tag{44}$$

$$= K(i^*_q\cos(e_\varphi) + i^*_d\sin(e_\varphi)) - \tau_L. \tag{45}$$

As simplification, the phase lag of the tracking filter is assumed proportional to the acceleration $e_\varphi = \frac{n_p}{v_1}\frac{\mathrm{d}}{\mathrm{dt}}\omega_M$. With a Taylor approximation of cos and sin by $\cos(x) = 1 - x^2$ resp. $\sin(x) = x$ for small position errors, and assuming proportional control $i^*_q = K_\omega(\omega^*_M - \omega_M)$, one obtains

$$\frac{\mathrm{d}}{\mathrm{dt}}\omega_M(J - \frac{n_p}{v_1}i^*_d) = -KK_\omega(\omega_M - \omega^*_M) + KK_\omega\frac{n_p^2}{v_1^2}\dot{\omega}^2(\omega_M - \omega^*_M) - \tau_L. \tag{46}$$

The condition for stability is therefore $\frac{\mathrm{d}}{\mathrm{dt}}\omega_M < \frac{v_1}{n_p}$ which is satisfied whenever v_1 is chosen high enough, for instance, according to (44) such that $\Delta\varphi_e < 1$ rad. This result shows that the impact of phase lag does not destabilize the speed controller. With $\tau_L = 0$, the sign of $\frac{\mathrm{d}}{\mathrm{dt}}\omega_M$ is always opposed to the control error $(\omega_M - \omega^*_M)$ and the controller converges well, for any parameters.

F. Comparison to asymptotic observers

The first claimed advantage is robustness to parametric uncertainties. In our comparison, which opposes the presented scheme to a reduced-order observer without parameter adaptation, it was found that the resulting estimation error is similar for given parameter deviations. However, the control scheme with estimator is not destabilized, errors of up to 30° are acceptable in steady state (stability with reduced performance). The observer, however, destabilized itself when such a large position error was present, as result, three to four

times lower errors are tolerable. Therefore, while open-loop robustness is similar, closed-loop robustness is better.

The second claimed advantage is dynamics. This implies the maximum possible acceleration before the scheme destabilizes. Giving comparative results is hard, see that, if the feedback gain of the observer is increased, higher accelerations can be tracked. This inherits drawbacks considering robustness and also the lowest possible speed. As advantage compared to our our scheme, an observer does not necessarily show a phase lag during acceleration, however, the presented drive operates well at its maximum acceleration (for instance, maximum torque without any additional inertia or load). The phase lag during acceleration could be removed by using a different filter, it is not directly related to the estimation scheme.

V. Highly Dynamical Operation

The position estimator itself only produces a small phase shift in transient operation, only depending on the time constant of the low pass filters for the current derivatives. In contrast, the phase shift produced by the filter (38) dominates. The maximum possible acceleration of the rotor $\dot{\omega}_M$ is known as

$$c_{max} = \frac{K\rho_{max}}{J}, \tag{47}$$

where c_{max} is the maximal acceleration, ρ_{max} the maximum current magnitude (the rated current in the testbench) and J is the rotor inertia of the synchronous machine. As soon as a load is attached to the machine, the inertia will be higher and the acceleration c lower. The parameter v_1 is designed according to (39) such that the phase shift caused by the second order tracking filter during acceleration is limited to 20° to guarantee stability.

This phase shift, however, will deteriorate the dynamical behavior as the current is not completely orthogonal to the flux, reducing the torque-per-ampere ratio. Assuming knowledge of the filter phase shift, it is possible to improve the dynamics. The rotor acceleration c is estimated from the speed reference ramp by $c = \frac{\mathrm{d}}{\mathrm{dt}}\omega_M^*$, assuming that the ramp is tracked, and the $d-$current is adapted to compensate for the misalignment. The feedforward compensation is

$$i_d^* = \tan\left(\Delta\varphi_e\right) i_q^* + i_{d0}^* = \tan\left(\frac{n_p \frac{\mathrm{d}}{\mathrm{dt}}\omega_M^*}{v_1}\right) i_q^* + i_{d0}^*, \tag{48}$$

where i_{d0}^* is the reference current to avoid zero $d-$current as described in sec. III.B. The measurements on Fig. 5 demonstrate the performance of this method. The machine can then operate at its maximum acceleration. Sensorless control is realized with the best possible dynamics.

VI. Experimental Results

The proposed sensorless control scheme is validated experimentally. A surface-mounted permanent magnet synchronous motor is used, whose parameters are shown on table I. The motor is powered by an industrial inverter. Furthermore, a load drive is attached. The sampling rate of the system is 16 kHz and the current is measured by closed-loop current transducers.

The field-oriented control scheme, consisting of cascaded PI control, the two estimators and the two filters, is shown in Fig. 2.

The current magnitude and angle derivatives $\dot{\rho}$ and $\dot{\phi}$ are low-pass filtered with a time constant of 0.5 ms. The current is limited to 6.3 A by the controllers and the $d-$current is $i_{d0}^* = 0.3$ A for all measurements except Fig. 5 (top).

For the estimation equation, the reference voltages given by the current controllers are applied. With the given configuration, speeds as low as 100 rpm in full load can be reliably reached.

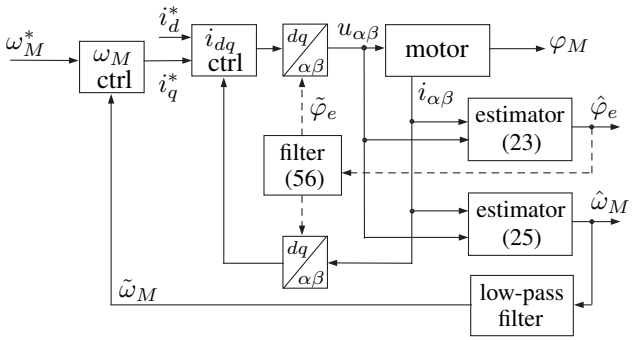

Fig. 2. Field-oriented encoderless control with the proposed estimators.

TABLE I
Nominal Parameters of the Synchronous Motor

Manufacturer & Model	Merkes MT5 1050
Rated Power P_N	2760 W
Rated Torque τ_{MN}	8.8 Nm
Rated Current	6.3 A
Rated Speed ω_{MN}	3000 rpm
Pole Pairs n_p	3
Rated Voltage U_N	400 V
Stator Inductance L_d, L_q	4.8, 7.2 mH
Stator Resistance R	0.86 Ω
Motor Constant K	0.236 Vs

In Fig. 3, steady-state is shown at $\omega_M = 100$ rpm resp. $\omega_M = 3000$ rpm and at nominal load $\tau_M = 8.8$ Nm. The estimated angle is well conditioned and only has an offset of about 7° from the measured angle. In steady-state, the error is proportional to the load. In low speed, the stator slotting can be seen, which is 20 slots per revolution.

Fig. 4 shows an acceleration from 300 to 3000 rpm at half nominal load $\tau_L = 4.4$ Nm. This setpoint change takes about 230 ms, and the current controller quickly reaches the motor current limit of 6.3 A. During this transient, the estimation error, mainly caused by the second-order filter (38), does not exceed the error limit of 10° as specified in the v_1, v_2 parameter design.

A similar scenario is shown on Fig. 5 (top), but here the acceleration is performed without load. The setpoint change is performed faster (150 ms) and has a max. slope of 31500 rpm/s. The estimation error becomes about 20° as the acceleration is doubled compared to Fig. 4 (see the time scale). The motor again operates at the current limit. The $d-$current feedforward compensator (52) generates a negative d-current of $i_d = -2.25A$ during the transient. It can be shown that the slope is 17% faster than without error compensation.

To confirm the good encoderless performance, Fig. 5 (bottom) shows the same setpoint change with an encoder. The dynamic behavior is about the same as in Fig. 5 (top).

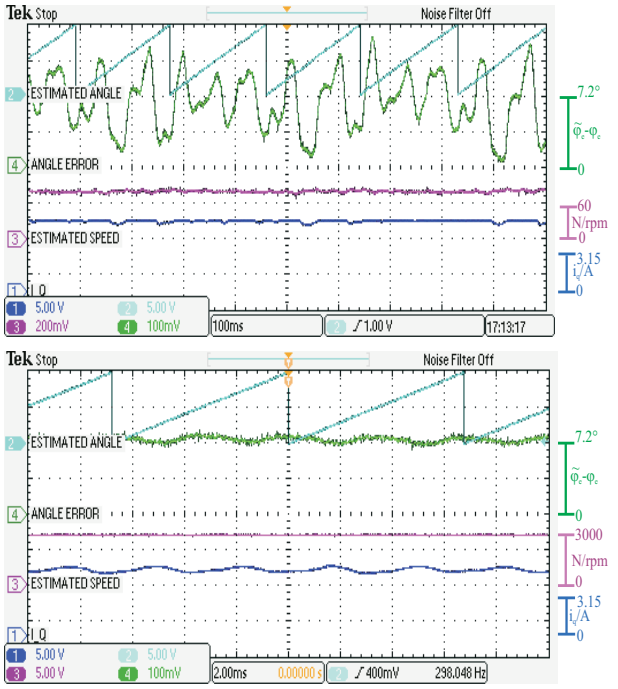

Fig. 3. Experimental results: Top: Encoderless control at 100 rpm and nominal load $\tau_L = 8.8$ Nm. Bottom: Encoderless control at 3000 rpm and nominal load $\tau_L = 8.8$ Nm. Cyan: estimated electrical angle $\tilde{\varphi}_e$ (π rad/div), Green: estimation error $\tilde{\varphi}_e - \varphi_e$ (0.01π rad/div), Magenta: estimated speed $\tilde{\omega}_M$ (300 rpm/div), Blue: current i_q in estimated frame (3.15 A/div).

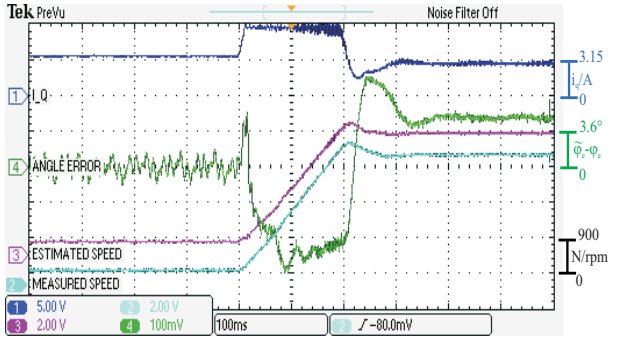

Fig. 4. Experimental results: Acceleration from 300 to 3000 rpm at half nominal load $\tau_L = 4.4$ Nm. Blue: current i_q in estimated frame (3.15 A/div), Green: estimation error $\tilde{\varphi}_e - \varphi_e$ (0.01π rad/div), Magenta: estimated speed $\tilde{\omega}_M$ (900 rpm/div), Cyan: measured speed (900 rpm/div).

VII. Conclusion

A very fast and robust position estimator based on a parallel-model estimator was introduced. The advantages of the use of a polar state representation were pointed out. The parametric robustness of the estimator, improved by avoiding asymptotic observers and speed estimation, was confirmed analytically and experimentally. Furthermore the scheme convinces by its high dynamic properties, which are presented in measurement results. The scheme is well suited for encoderless control of PMSMs at nonzero speed, especially as it is quite easy to implement.

References

[1] J.R. Frus and B.C. Kuo, "Closed-loop control of step motors using waveform detection," in *Proc. Int. Conf. Stepping Motors and Systems*, pp. 77-84, 1976.

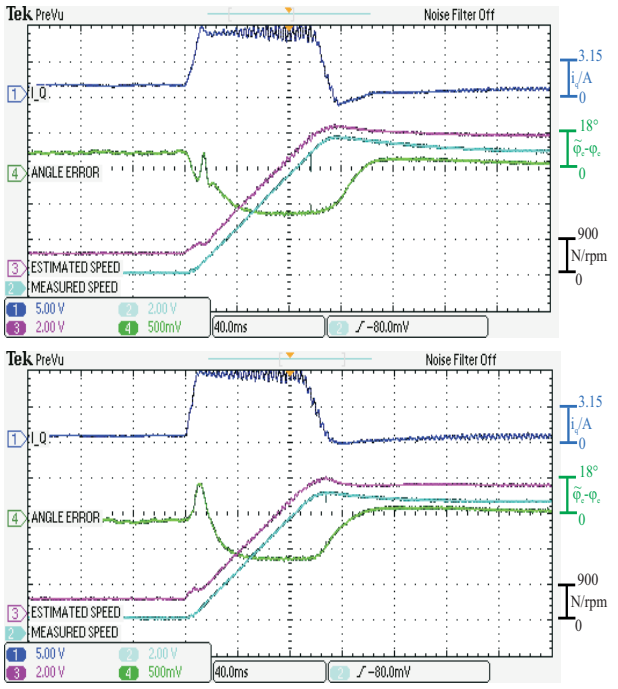

Fig. 5. Experimental results: Acceleration from 300 to 3000 rpm without load. Top: proposed encoderless control scheme with i_d error compensation (52), bottom: encoder-based control as reference. Blue: current i_q in estimated frame (3.15 A/div), Green: estimation error $\tilde{\varphi}_e - \varphi_e$ (0.05π rad/div), Magenta: estimated speed $\tilde{\omega}_M$ (900 rpm/div), Cyan: measured speed (900 rpm/div).

[2] P.P. Acarnley and J.F. Watson, "Review of position-sensorless operation of brushless permanent-magnet motors," in *IEEE Trans. Ind. Electron.*, vol. 53, no. 2, pp. 352-362, 2006.
[3] A. Consoli, F. Russo and A. Testa, "Low- and zero-speed sensorless control of synchronus reluctance motors," *IEEE Trans. Ind. Appl.*, vol. 35, no. 5, pp. 1050–1057, 1999.
[4] M. Schroedl, "Sensorless control of AC machines at low speed and standstill based on the "inform" method," *IEEE Trans. Ind. Appl.*, Vol. 34, pp. 270-277, 1996.
[5] C. Silva, G.M. Asher and M. Sumner, "Hybrid rotor position observer for wide speed-range sensorless PM motor drives including zero speed," *IEEE Trans. Ind. Electron.*, vol. 53, no. 2, pp. 373-378, 2006.
[6] G. Zhu, A. Kaddouri, L. A. Dessaint, and O. Akhrif, "A nonlinear state observer for the sensorless control of a permanent-magnet AC machine," *IEEE Trans. Ind. Electron.*, vol. 48, no. 6, pp. 1098-1108, 2001.
[7] J. Lee, J. Hong, K. Nam, R. Ortega, L. Praly and A. Astolfi, "Sensorless control of surface-mount permanent-magnet synchronous motors based on a nonlinear observer," in *IEEE Trans. Power Electr.*, vol. 25, no. 2, pp. 290-297, 2010.
[8] T. Furuhashi, S. Sangwongwanich, and S. Okuma, "A position-and-velocity sensorless control for brushless dc motors using an adaptive sliding mode observer," *IEEE Trans. on Ind. Electron.*, vol. 39, pp. 89-95, 1992.
[9] M. Bodson and J. Chiasson, "A comparison of sensorless speed estimation methods for induction motor control," *Proc. American Control Conf.*, pp. 3076–3081, 2002.
[10] H.S. Yoo and I.J. Ha, "A polar coordinate-oriented method of identifying rotor flux and speed of induction motors without rotational transducers," *IEEE Trans. Control Sys. Tech.*, Vol. 4, No. 3, pp. 230–243, 1996.
[11] J-F. Stumper and R. Kennel, "Field-oriented control of a speed-sensorless induction motor for the complete speed range using a nonlinear observer," in *Proc. of the IEEE Int. Symp. on Sensorless Control for Electrical Drives*, 2011.
[12] J. Liu, T. Nondahl, P. Schmidt, S. Royak and M. Harbaugh, "Equivalent EMF based position observers for sensorless synchronous machines," *Proc. of the Appl. Power Electronics Conf. and Exp.*, pp. 425–432, 2010.
[13] R. Castro-Linares, J. Alvarez-Gallegos and E. Alvarez-Sánchez, "Angular velocity and position control of a permanent magnet stepper motor," *Proc. of the European Control Conf.*, 2003.
[14] D. Paulus, J-F. Stumper, P. Landsmann and R. Kennel, "Robust encoderless speed control of a synchronous machine by direct evaluation of the back-EMF angle without observer," in *Proc. of the IEEE Int. Symp. on Sensorless Control for Electrical Drives*, pp. 8–13, 2010.
[15] H. Sira-Ramírez and S.K. Agrawal, *Differentially flat systems*. New York: Marcel Dekker, 2004.